Determination of the Interaction and Pharmacological Modulation of MCHR1 Signaling by C Terminus of MRAP2 Protein

Meng Wang (✉ 2440325367@qq.com)
Shanghai 9th Peoples Hospital Affiliated to Shanghai Jiaotong University School of Medicine
https://orcid.org/0000-0003-0221-0653

Yue Zhai
Tongji University

Xiaowei Lei
Tongji University

Jing Xu
Tongji University

Bopei Jiang
Tongji University

Zhe Kuang
Tongji University

Yanbin Fu
Shanghai 9th Peoples Hospital Affiliated to Shanghai Jiaotong University School of Medicine

Cong Zhang
Shanghai 9th Peoples Hospital Affiliated to Shanghai Jiaotong University School of Medicine

Shangyun Liu
Shanghai 9th Peoples Hospital Affiliated to Shanghai Jiaotong University School of Medicine

Shan Bian
Tongji University

Xiao-Mei Yang
Tongji University

Li-Na Jin
Shanghai Changzheng Hospital

Qingfeng Li
Shanghai 9th Peoples Hospital Affiliated to Shanghai Jiaotong University School of Medicine

Chao Zhang
Shanghai 9th Peoples Hospital Affiliated to Shanghai Jiaotong University School of Medicine

Research Article

Keywords: MRAP2, GPCR, Melanin-concentrating hormone, pharmacological regulation

Posted Date: October 14th, 2021

DOI: https://doi.org/10.21203/rs.3.rs-829492/v2

Version of Record: A version of this preprint was published at Frontiers in Endocrinology on March 4th, 2022. See the published version at https://doi.org/10.3389/fendo.2022.848728.

Abstract

Background: Melanin concentrating hormone (MCH), an orexigenic neuropeptide, is primarily secreted by the hypothalamus and acts at its receptor, the melanin-concentrating hormone receptor 1 (MCHR1), to regulate energy homeostasis and body weight. The Melanocortin Receptor Accessory Protein 2 (MRAP2), a small single transmembrane protein broadly expressed in multiple tissues, has been defined as a vital endocrine pivot of five melanocortin receptors (MC1R-MC5R) and several other GPCRs in the regulation of central neuronal appetite and peripheral energy homeostasis. However, the regulatory and relationship between MCHR1 and MRAP2 is unknown.

Results: In this study, we show that MRAP2 interacts with MCHR1 and suppresses MCHR1 signaling in vitro. We also identified the C-terminal domains of MRAP2 protein required for pharmacological modulation of intracellular Ca2+ cascades and membrane transport.

Conclusions: These findings elucidated the broad regulatory profile of MRAP2 protein in the central nervous system and may provide implications for the modulation of central MCHR1 function in vivo.

Introduction

Hypothalamus is one of the most important neuronal cores for the integration of a variety of physiological signals from the brain and the periphery to modulate secretion of multiple peptidic pituitary hormones involved in maintaining energy homeostasis and proper feeding behavior. Melanin concentrating hormone (MCH) is a cyclic peptide primarily expressed in hypothalamus, which is involved in regulating energy balance (Bohlooly et al., 2004). MCH acts through two G protein-coupled receptors, MCHR1 and MCHR2 (Zhang et al., 2014). MCH binds to MCHR1 (also called SLC-1 or GPR24) with high affinity and it has been shown to couple to three Gα proteins: Gi, Go, and Gq. In the hippocampus and frontal cortex, MCH preferably signals through the Gq-coupled pathway, activates MCHR1 and increases intracellular Ca2 + level (Antal-Zimanyi and Khawaja, 2009). Deletion of MCHR1 creates a phenotype of weight loss and resistance to diet-induced obesity characterized by hyperphagia, hyperactivity and hypermetabolism (Kowalski et al., 2006), indicates a central role of MCHR1 in stimulating food intake and increasing body weight in rodents (Elliott et al., 2004).

Melanocortin receptor accessory proteins (MRAPs) include melanocortin receptor accessory protein 1 (MRAP1) and melanocortin receptor accessory protein 2 (MRAP2). MRAP2 is highly expressed in the hypothalamus, containing the paraventricular nucleus (PVN), and has been linked to mammalian obesity, recently (Asai et al., 2013; Chan et al., 2009). It has been shown that MRAP2 potentiates melanocortin-4 receptor (MC4R) signaling in several species (Asai et al., 2013; Huszar et al., 1997; Sebag et al., 2013) and plays a key role in GPCR signaling to regulate the dynamic neuronal appetite and food intake. Both MRAP2 and MC4R KO mice develop severe obesity syndrome in human and murine models. Notably, MC4R KO mice show a hyperphagia phenotype that is absent in MRAP2 knockout mice. Given that MRAP2 also regulates the activity of several other metabolic-related GPCRs besides MC4R, such as PKRs

(Chaly et al., 2016), OX1R (Rouault et al., 2017a) and GHSR1α (Srisai et al., 2017), and that the regulatory regions for these GPCRs are specific (Rouault et al., 2017a; Rouault et al., 2020a), we speculate that the absence of hyperphagia in MRAP2 knockout mice could arise from the coordinated modulation of the MRAP2 protein on multiple endogenous metabolic-related GPCR signaling pathways.

In this study, we investigated the regulatory profile of the MRAP2 protein on the trafficking and signaling of MCHR1. MRAP2 interacted with MCHR1 in vitro and the regulation of MCHR1 signaling required distinct functional regions. Collectively, we observed the simultaneous inhibitory effect of MRAP2 on the orectic MCHR1 signaling and established that MRAP2 could not only suppress appetite by inhibiting MCHR1 signaling. Our data not only identified MCHR1 as novel metabolic-associated GPCR target of the MRAP2 protein, but also elucidated the complex endocrine network of GPCR signaling which may explain the composite metabolic phenotypes of MRAP2 deficiency.

Results

Correlation of MCHR1 and MRAP2 co-expression

We developed a custom script to interrogate the co-expression correlation of MCHR1 and MRAP1 or MRAP2 in 1698 human or mice bulk RNA-seq samples of central nervous system (including 1000 human whole brain samples, 435 mice whole brain samples, 202 human hypothalamic samples and 61 mouse hypothalamic samples) from the Genotype-Tissue Expression (GTEx) project database and all RNA-seq and ChIP-seq sample and signature search (ARCHS4) database. As shown in Fig. 1A-B, a few number of cells co-expressed MCHR1 and MRAP1 in bulk RNA-seq datasets, which showed a low correlation (mean_cor = 0.2) between MCHR1 and MRAP1. While the number of co-expressing MCHR1 and MRAP2 is comparatively larger, which revealed high correlation (mean_cor = 0.6) between MCHR1 and MRAP2. In order to better explore the effect of MCHR1 on the phenotype of MRAP2 null mice and in view of the accuracy and specificity of single-cell RNA sequencing, we next analyzed the co-expression correlation of MCHR1 and MRAP2 in 28,320 cells of 20 mice from 4 published single-cell RNA-seq datasets of Gene Expression Omnibus (GEO) database. We found that MCHR1 and MRAP2 have lots of number of co-expressed cells in single-cell sequencing data as well (Fig. 1C). The average correlation between MCHR1 and MRAP2 in the 4 datasets is relatively large (mean_cor = 0.5).

MCHR1 and MRAP2 both play a critical role in energy homeostasis. Therefore, we analyzed the cell number ratio change of MCHR1 and MRAP2 under different metabolic condition to explore their metabolic relevance. The results showed that MCHR1 and MRAP2 had consistent cell ratio shift in HFD group compared to control, which were both significantly up-regulated (Fig. 1D). Furthermore, we found that MRAP1, MRAP2 and MCHR1 can be enriched in some energy metabolism pathways. Among them, MRAP1 and MRAP2 are both related to the binding of neuropeptides and GPCR signaling pathways. More importantly, GO(Gene Ontology) functional analysis exhibits that MCHR1 and MRAP2 both attributed to regulation of feeding behavior (Fig. 1E). These results all preliminarily indicate that MCHR1 and MRAP2 may have a synergistic effect on regulating energy metabolism in central nervous system.

Tissue-distribution and interaction of MCHR1 with MRAP1 or MRAP2

To characterize mRNA expression profiles of MCHR1, MRAP1 and MRAP2 in vivo, Our RT-PCR analysis was extended to 14 tissues from mice. MRAP1 and MRAP2 show universal expression in different tissues compared to MCHR1 (Fig. 2A). However, the expression of MCHR1, MRAP1 and MRAP2 show consistency in some organizations, which are all highly expressed in the brain, cerebellum and eye. These results suggest that the MCHR1, MRAP1 and MRAP2 may function together in vivo.

This finding provides evidence for co-expression of these proteins, to further determine whether MRAP2 could interact with MCHR1 protein, we performed co-immunoprecipitation (Co-IP) assays in HEK293T cells transfected with 3HA-MCHR1 and 2Flag-MRAP1 or 2Flag-MRAP2. As shown in Fig. 2B, MCHR1 did not co-purify with MRAP1 whereas co-purified with MRAP2 (Fig. 2C). Besides, we found that neither MCHR1 or MRAP proteins were observable when the purification was executed with protein A + G agarose beads only (without immunoprecipitation antibody) (Fig. 2B-C: the first two lanes in IP group). Western blot on cell lysates transfected with MCHR1, MRAP1 or MRAP2 alone was also performed to affirm that the bands observed for those proteins matched the ones detected in the IP group(Fig. 2B-C: the right half of lysate side).

Next, to further assess the ability of MCHR1 to form a functional protein complex with MRAP2 but not MRAP1 in live cells, we performed bimolecular fluorescence complementation (BiFC) assays. To achieve this goal, we generated MCHR1 constructs fused to YFP-F1 fragment in the C-terminus, while the C-terminal of MRAP1 or MRAP2 was fused to the complementary YFP-F2 fragment and Flag tag (Fig. 2D,2H). As we expected, the expression of MRAP1-Flag-F2 with MCHR1-F1 alone did not exhibit any fluorescence (Fig. 2E-G). However, YFP fluorescence was detected when co-transfected of MCHR1-F1 and MRAP2-Flag-F2 (Fig. 2I-K), suggesting that MRAP2 but not MRAP1 could form a functional complex with MCHR1, because the emission of a fluorescent YFP molecule requires the close proximity of YFP-F1 and YFP-F2 fragments.

Modulation of the surface translocation of MCHR1 by MRAP2 proteins

The trafficking of several GPCRs has been shown to be modulated by MRAP2 (Chaly et al., 2016; Chan et al., 2009; Rouault et al., 2017a; Srisai et al., 2017). To test whether MRAP2 alters the membrane translocation of MCHR1, we performed an Enzyme-linked Immunosorbent Assay (ELISA) to measure the cell surface receptors expression quantitatively. The 3HA tag was added to the N-terminus of MCHR1 and the construct was then expressed with or without MRAP2 in HEK293T cells. To determine the effect of MRAP2 on the expression of MCHR1, 3HA-MCHR1 and either MRAP2 or RAMP3 (control) at different receptor to accessory ratios (from 1:0 to 1:9) were transfected to cells. MCHR1 surface expression was detected at OD 450 nm after the addition of the HA antibody and substrate with or without cell lysis blocking. Cell numbers were measured at OD 595 nm and normalized by cell normalization stain, Janus

Green. We showed that MRAP2 significant decreased the surface expression of MCHR1 compared to the control group (Fig. 3A). In general, as the ratio increased, the difference between the MRAP2 group and the control group increased (Fig. 3B). These results indicate that more than two molecules of MRAP2 interact with MCHR1, which was consistent with the results of OX1R studies. Our results showed that, at a 1:9 ratio, while MRAP2 decreased the maximal surface density of MCHR1 by > 60%, the total expression of MCHR1 was only reduced by 20% when MRAP2 existed compared to the control group (Fig. 3C). GFP-MCHR1 alone, or with MRAP2 or RAMP3 was transfected to cells to further visualize the impact of MRAP2 on MCHR1 location. We can see from the images that expression GFP-MCHR1 only or with RAMP3, GFP fluorescence was mainly present at the plasma membrane (Fig. 3D: the left and right panel), whereas GFP-MCHR1 was mostly retained in the intracellular compartment in the presence of MRAP2, which is consistent with the ELISA results. (Fig. 3D: the middle panel).

Repression of the surface expression of MCHR1 by specific regions of MRAP2

These preferential localizations suggested that MRAP2 was involved in MCHR1 trafficking to the plasma membrane. But the functional domain of MRAP2 on MCHR1 trafficking needed to be further explored. Several studies have shown that specific regions of MRAP2 are not required for the regulation of different GPCRs (Rouault et al., 2017a; Rouault et al., 2020b). To find the regions of MRAP2 that were necessary for its inhibition on MCHR1 trafficking, a series of MRAP2 mutants were generated, in which the N-terminal fragments were deleted and the C-terminal fragments were truncated (Fig. 3F). The regions of mouse MRAP2 that were truncated were same as the human MRAP2 in a previous study (Rouault et al., 2017a), since we conducted an amino acid sequence comparison in mice and human MRAP2, and found that they are high conservative, especially their TM area are completely consistent. (Fig. 3E). Using ELISA experiments, we explored the effect of each MRAP2 mutant on the surface expression of MCHR1. Our results showed that the deletion of the whole C-tail caused a loss of MRAP2 function on MCHR1 surface expression (Fig. 3G).

To explore whether the effect of these MRAP2 mutants on receptor membrane transport was caused by the disappearance of their interaction, we performed Co-IP experiments to verify the interplay between each MRAP2 mutant with MCHR1. The results showed that each MRAP2 mutant still exhibited interactions with MCHR1 (Fig. 4). Here, TM dimerization domain was retained in all MRAP2 constructs, with reference to Chen et al (Chen et al., 2020). This is important because these authors identify the TM as the dimerization domain. By retaining it the MRAP2 protein is allowed to dimerize.

Co-localization of MRAP2 mutants with MCHR1

Next, we also performed co-immunofluorescence to investigate the role of the identified functional regions of MRAP2 on MCHR1 trafficking. Different MRAP2 mutants tagged with 2Flag (WT, Δ4–11, Δ12–25, Δ26–35, Δ36–45, Δct, t97, t118 and t143) were co-transfected with 3HA-MCHR1 into cells. The results showed that the nonfunctional MRAP2 mutants were all expressed (Fig. 5), meaning that the loss of

activity of these mutants was not due to lack of expression. Moreover, the coIF results confirmed again that each MRAP2 mutant had interactions with MCHR1.

The influence of MCHR1 signaling by the functional domains of MRAP2

It was previously shown that MRAP2 inhibited the signaling of OX1R and PKR1 (Rouault et al., 2017a). Based on this, we detected whether the regions of MRAP2 required for the inhibition of MCHR1 were same. To achieve this goal, we transfected HEK293T cells with MCHR1 in the presence of WT MRAP2 or MRAP2 mutants at a 1:9 ratio and measured the Ca2 + influx of MCHR1 via the CRE-luciferase reporter assay. The results showed that MRAP2 strongly decreased the efficacy of MCH (Fig. 6A-H: the blue curve). Moreover, MRAP2-Δ12–45 retained a significant inhibitory action on MCHR1 signaling (Fig. 6B-D: the black curve), while the inhibition of MRAP2 on MCHR1 signaling was almost completely reversed when transfected with MRAP2-Δ4–11 or the C-terminal truncations of MRAP2 (Fig. 6A, E-H: the black curve). Moreover, as we can see in Table1, the sensitivity of MCHR1 to MCH was reduced to varying degrees by adding MRAP2 or MRAP2 truncated constructs. Especially with the addition of mRAP2 Δ12–25 and Δ36–45 mutants, the EC50 value changed by an order of magnitude, from 10-8M to more than 10-7M.

Table 1
Statistical analysis of MCHR1 in the presence of different MRAP2 mutants in response to MCH.

Data statistics of Fig. 6A-H	LogEC50	P value comparison	
		vs. receptor alone	vs. MRAP2 WT
MCHR1 alone	-8.149 ± 0.10	-	< 0.0001
MCHR1:MRAP2 WT	-7.061 ± 0.40	< 0.0001	-
MCHR1:MRAP2 Δ4–11	-7.242 ± 0.19	< 0.0001	< 0.0001
MCHR1:MRAP2 Δ12–25	-6.765 ± 1.15	< 0.0001	0.9803
MCHR1:MRAP2 Δ26–35	-7.551 ± 0.31	< 0.0001	< 0.0001
MCHR1:MRAP2 Δ36–45	-6.643 ± 0.43	< 0.0001	0.8704
MCHR1:MRAP2 Δct	-7.515 ± 0.54	< 0.0001	< 0.0001
MCHR1:MRAP2 t97	-7.338 ± 0.68	< 0.0001	< 0.0001
MCHR1:MRAP2 t118	-7.593 ± 0.63	< 0.0001	< 0.0001
MCHR1:MRAP2 t143	-7.599 ± 0.46	< 0.0001	< 0.0001
Values were expressed as the mean ± S.E.M. of at least three independent experiments. Two-way ANOVA with Tukey post-test was applied in the statistical analysis.			

In addition, we also performed competitive inhibition experiments (Fig. 6I-P). We added different concentrations of MCHR1 antagonist (SNAP-94847) in the presence of EC80 MCH (10 − 7 M) to observe the effect of MRAP2 mutants on MCHR1. We found that, consistent with the results observed in Fig. 6A-H, the inhibition of MCHR1 signaling relied on the 4–11 amino acids and the C-terminus of MRAP2 (Fig. 6I, M-P). Except for the addition of Mrap2 Δ 26–35 and T143, IC50 of MCHR1 has a slight decrease, other variants all increase the sensitivity of MCHR1 to the inverse agonist, but in general IC50 values were not significantly different (Table 2). In short, these results indicated that the trafficking and signaling of MCHR1 were both inhibited by MRAP2, suggesting that different MRAP2 regions were involved in regulating distinct GPCR (Fig. 6Q).

Table 2
Statistical analysis of MCHR1 in the presence of different MRAP2 mutants in response to the antagonist of MCHR1.

Data statistics of Fig. 6I-P	LogIC50	P value comparison	
		vs. receptor alone	vs. MRAP2 WT
MCHR1 alone	-8.584 ± 0.53	-	< 0.0001
MCHR1:MRAP2 WT	-7.752 ± 0.68	< 0.0001	-
MCHR1:MRAP2 Δ4–11	-7.977 ± 0.57	< 0.0001	< 0.0001
MCHR1:MRAP2 Δ12–25	-8.451 ± 0.89	< 0.0001	0.2763
MCHR1:MRAP2 Δ26–35	-9.278 ± 0.57	< 0.0001	0.6027
MCHR1:MRAP2 Δ36–45	-8.408 ± 0.68	< 0.0001	0.2858
MCHR1:MRAP2 Δct	-7.641 ± 0.94	0.0002	< 0.0001
MCHR1:MRAP2 t97	-8.251 ± 0.69	0.0002	< 0.0001
MCHR1:MRAP2 t118	-8.314 ± 0.69	< 0.0001	0.4248
MCHR1:MRAP2 t143	-8.683 ± 0.51	< 0.0001	0.0875
Values were expressed as the mean ± S.E.M. of at least three independent experiments. Two-way ANOVA with Tukey post-test was applied in the statistical analysis.			

Discussion

MRAP2 is an essential accessory factor for the regulation of melanocortin receptor family. And melanocortin receptor 4 (MC4R) is the first GPCR related to energy homeostasis that was thought to be regulated by MRAP2. MRAP2 potentiates MC4R signaling in vitro and the deletion of MC4R and MRAP2 both develop severe obesity in vivo (Asai, 2013; Sebag et al., 2013). MRAP2 was successively confirmed to be involved in the regulation of several other non-melanocortin receptors related to metabolism preprokineticin receptor family (PKRs) (Chaly et al., 2016), pro-orexin receptor 1 (OX1R) (Rouault et al.,

2017a), growth hormone secretagogue receptor 1a (GHSR1a) (Rouault et al., 2020b; Srisai et al., 2017). In this study, we further proves that MRAP2 is a wide modulator of GPCRs, it's promising that more receptors will be identified as MRAP2 partners in the future.

MRAP2 shows short N-terminus which contain glycosylation sites, and forms special antiparallel dimer structurally. The orthologs of MRAP1 have identical N-terminal and transmembrane (TM) regions, whereas the C-terminal portion is various (Webb and Clark, 2010). Unlike MRAP1, the entire sequence of MRAP2 is high conservative including the C-termini, which suggests the C-tail of MRAP2 perhaps act some important functions (Rouault et al., 2017b). It has been proved that distinct regions of MRAP2 take part in the inhibition of trafficking and signal transduction of PKR1 and OX1R independently (Rouault et al., 2017a). Recently, the influences of MRAP2 on the Gαq and β-arrestin pathways were also independent relevant different regions of MRAP2 described by Rouault and coworkers (Rouault et al., 2020b). In our study, we find that the C-terminus are required for MRAP2 to repress the surface expression and inhibit the activity of MCHR1, while for N-terminal of MRAP2, only residues 4–11 exhibit important roles for signaling of MCHR1. All in all, the C-terminus seems to play a greater role in regulating MCHR1. It also should be noted that MRAP2-Δ4–11, which we cite along the C-terminal truncation of MRAP2 as those involved in inhibiting MCHR1 expression, may act by a different mechanism. As is known, there is a glycosylated asparagine at position 9, which if inactivated o Vr deleted inhibits the function of MRAP2. Also, we show that the interaction between MCHR1 and MRAP2 still occurs after deletion and mutation of the C-terminal and N-terminal, respectively. This makes sense, because it has been reported that the TM region of Mrap2 is the smallest region for Mrap2 to form dimer(Chen et al., 2020), which indicates that the TM region is the key region for the interaction with GPCR and is relatively independent of the region for signal activity and membrane transport.

So far, all GPCRs regulated by MRAP2 and related to energy balance and food intake have a common feature, that is, highly expressed in the hypothalamus as same as MRAP2. MRAP2 could regulate the sensitivity of a series of hypothalamic neurons to their neuropeptides, such as α-MSH, prokineticins, orexins and Ghrelin. MCH is also abundant in hypothalamus. Leptin appears to be an important biological signal in this MRAP2-GPCR system through which α-MSH/MCH additively or synergistically interacts to effect food intake and body weight. When leptin binds to its receptors on POMC neurons, POMC releases α-MSH (α-melanocortin stimulating hormone), which activates downstream of MC4R to transmit satiety signals (Ranadive and Vaisse, 2008), and MRAP2 interacts w-ith MC4R and potentiates its activity, thereby inhibits food intake. Leptin reduced the expression of MCHR1 and Lepob/ob mice significantly increased in MCHR1 expression in the hypothalamus (Kokkotou et al., 2001). MCH and α-MSH have opposing effects. MCHR1 expression is decreased due to MCH is repressed by leptin. Functionally, although MRAP2 inhibits surface expression of MCHR1 it is unclear how this would affect physiological processes of food intake. We assume that MRAP2 inhibits MCHR1 signaling, which may lead to food intake reduced, which part needs to be further confirmed in vivo. In short, our work reveals some of MRAP2 mechanisms and the MRAP2 functional domains involved in GPCR surface expression and activity. The identification of MRAP2 interacting partners shows some novel aspects of physiology and may benefit to develop drugs that target these pathways in future studies.

Methods And Materials

In silico analysis of bulk and single transcriptome of MCHR1, MRAP1 and MRAP2 expression

Human bulk RNA sequencing data were downloaded from The Genotype-Tissue Expression (GTEx) project (https://www.gtexportal.org/) and mouse RNA sequencing datasets were downloaded from all RNA-seq and ChIP-seq sample and signature search (ARCHS4) database (https://amp.pharm.mssm.edu/archs4/). Datasets of mouse cerebric and hypothalamic single-cell RNA-seq were GSE74672, GSE87544, GSE130597 and GSE125065, which are downloaded from Gene Expression Omnibus (GEO) DataSets.

For bulk RNA sequencing data analysis, Fragments Per Kilobase per Million mapped fragments (FPKM) was utilized to normalize the expression level of each mRNA transcript. Next, we respectively analyzed the samples of whole brain and hypothalamus from humans and mice. We calculated Pearson's correlation coefficient between MCHR1 and MRAP1 or MRAP2 expression value across all samples. For single cell RNA-seq analysis, all datasets were filtered and excluded low-quality cells that had unique feature counts less than 200. The co-expression of cell number between MRAP2 and MCHR1 positive neuronal populations were calculated. Next, Pearson's correlation coefficient was calculated between the expression value of MRAP2 and MCHR1 across all cells.

To calculate the changes in MRAP2 and MCHR1 expression under high-fat diet condition, we counted the proportion of cells expressing this gene in the expression profiles of high-fat diet and normal diet respectively. And tested the significance of the differences using fisher's exact test. In order to explore the pathways in which these genes are involved, we did GO pathway enrichment analysis using clusterProfiler R package.

Reagents, plasmids, and antibodies

MCHR1, MRAP1 and MRAP2 were alll amplified from wild type BL/C57 mice cDNA. All PCR products were ligated into pcDNA3.1(+) vector and the constructs were all verified by sanger sequencing. Melanin concentrating hormone (MCH) was purchased from BACHEM. SNAP-94847 (MCHR1 antagonist) was purchased from MCE. In this study, anti-mouse HA monoclonal antibody (Sigma-Aldrich, MO, USA), Anti-mouse Flag monoclonal antibody (ABclonal Biotech Co., Ltd, Wuhan, China), Anti-mouse IgG antibody (ABclonal Biotech Co., Ltd, Wuhan, China) and HRP-conjugated antibodies against mouse (ABclonal Biotech Co., Ltd, Wuhan, China) were used.

Cell culture and transfection

HEK293T cells were cultured in DMEM medium (high glucose) supplied with 10% FBS and 1% penicillin–streptomycin (P/S). And cells were incubated in 37°C cell incubator consisting of 5% CO2. Transfection was conducted using P-PEI reagent according to the manufacturer's protocols. The total transfected amount of plasmids was kept identical in each group by adding empty pcDNA3.1 vector.

Tissue expression analysis

RT-PCR in this study was performed as previously described (Agulleiro et al., 2010). Briefly, cDNA was synthesized by extracting RNA from 14 mouse tissues (heart, liver, spleen, lung, stomach, pancreas, fat, kidney, brain, cerebellum, eye, thorax, spinal cord and genital gland). All PCR products were separated on 1.5% agarose gel and β-actin as internal control was also carried out. Primers used in this study were all synthesized from GENEWIZ and the primer sequences of mMCHR1, mMRAP1, mMRAP2 and mβ-actin are listed as below. mMCHR1_fw: ATCACTGCTGCGTACGTGAA; mMCHR1_rev: TCACCCTCTTTGTCCGAAGC; mMRAP1_fw: CTGAAAGCCAACAAGCATTCCA; mMRAP1_rev: CCGACCAGGACATGTAGAGC; mβ-actin _fw: GCCTTCCTTCTTGGGTATGGA; mβ-actin_rev: ACGGATGTCAACGTCACACT.

Western blot and co-immunoprecipitation

Proteins were extracted 24–36 h after transfection and then incubated with mouse anti-HA or mouse anti-Flag antibody at 1:5000 dilution overnight at 4°C. Next day, protein A + G beads (Beyotime, Shanghai, China) were added and rotated at 4°C for 4 h. Finally, beads were re-suspended in protein loading buffer after 3 washes and boiled for 15 min. Samples were run on 12% SDS-PAGE gels and mouse anti-FLAG antibody was used for detecting MRAP1/MRAP2 in MCHR1 co-immunoprecipitation experiments. Images were captured by ImageQuant 4000.

Bimolecular Fluorescence Complementation Assay (BiFC) and co-immunofluorescence

HEK293T cells seeded on poly-L-lysine pretreated coverslips and transfected with MCHR1-F1 and MRAP1-Flag-F2 or MRAP2-Flag-F2. The next day, cells were fixed with 4% PFA Fix Solution for 20 minutes. Cells were incubated with anti-FLAG antibody (Cell Signaling) at 1:5000 for 2 h at room temperature to detect MRAP1 and MRAP2. Then washed 3 times and incubated with 1:5000 secondary antibody Alexa Fluor594 (Abcam) for 2 h at room temperature. To detect membrane translocation of MCHR1 in presence of MRAP2, we transfected GFP-MCHR1 and MRAP2 or RAMP3 in a ratio of 1: 9 into cell, with no antibody treated. In order to observe co-fluorescence of MCHR1 and MRAP2 chimeras, 3HA-MCHR1 and each 2xFLAG MRAP2 chimera were transfected transiently into cells. Cells were incubated with both anti-HA and anti-FLAG antibody (Cell Signaling) at 1:5000 for 2 h at room temperature. Then washed 3 times and incubated with both 1:5000 secondary antibody Alexa Fluor488 (Abcam) and Alexa Fluor594 (Abcam) for 2 h at room temperature.

Coverslips were fixed with nail polish on the glass slide containing ProLong (R) Gold Antifade with DAPI Molecular Probes (Cell Signaling). Imaging was performed using a 63X oil objective with laser-scanning Zeiss confocal microscopy (LSM880).

Enzyme-linked immunosorbent assay (ELISA)

HEK293T cells were seeded in 12-well plates and transfected with MCHR1 and MRAP2 (1:0 to 1:9 ratio receptor to MRAP2). Upon 24-36h transfection, ELISA were performed as previous described (Jones et al.,

2007). Cells were fixed 20 min with 4% PFA after 3 washes and then blocked with 5% milk in PBS for 30 min at room temperature. Next, cells were incubated with mouse anti-HA monoclonal antibodies (1:2000) for 2h, following HRP-conjugated secondary antibodies against mouse (1:2000) incubation for 2h at room temperature. After incubating with TMB solution for 15 min, the reaction was stopped with 5% sulfuric acid. And the absorbance was read at 450 nm on Spectramax M5 multimode plate reader.

Ca2 + luminescent assay

HEK293T cells were cultured in 24-well plates and different MRAP2 mutants were co-transfected along with MCHR1, NFAT (firefly luciferase) and pRL-TK (renilla luciferase) reporter vectors into HEK293T cells via P-PEI according to the manufacturer's instructions. After 24-36h transfection, old medium was removed and different concentrations of MCH (from 10^{-6} to 10^{-11}M) in DMEM supplemented with 0.1% BSA were added in cell and incubated for 9h at 37°. For competitive inhibition test, concentration of SNAP-94847 (MCHR1 antagonist) ranged from 10^{-6} to 10^{-11}M was added in HEK293T cells supplemented with 2×10^{-9}M (EC80) MCH.

Dual-luciferase reporter gene assays in this study were conducted using Dual-Glo kits (Promega, WI, USA) according to the manufacturer's instructions. Luciferase activities were tested by Spectramax M5 multimode plate reader. Firefly luciferase values were normalized to Renilla luciferase values for relative quantification.

Sequence homology comparison

DNAMAN software was utilized to compare the amino acid sequence similarity of human and mouse MRAP2. Distinct colors highlighted the similarity score of various amino acids, in which the Red represented 100% consistency between sequences; blue indicated the amino acids at this position were not conserved, which got a similarity score between 0 to 33.

Statistic analysis

All experiments in this study were repeated at least three times. Data were analyzed by the Graphpad Prism6 software. Pharmacological curves were carried out by the log(agonist) vs. response equation (Y = Bottom+(Top-Bottom)/(1 + 10^((LogEC50–X)))) (X: log(agonist); Y: response values) method. One-way ANOVA with Tukey post-test were applied to measure significance between groups and results were shown as mean ± SEM. The tests were performed with a nominal significant level of *p < 0.05, **p < 0.01, ***p < 0.001 and ****p < 0.0001.

Declarations

Ethics approval and consent to participate

Not applicable.

Consent for publication

Not applicable.

Availability of data and materials

All data generated or analysed during this study are included in this published article [and its supplementary information files].

Competing interests

The authors declare that they have no competing interests

Funding

This work was supported by grants from the National Key Research and Development Program of China (Grant No. 2017YFA0103902 & 2019YFA0111400), the Natural Science Foundation of China (31771283), the Innovative Research Team of High-level Local Universities in Shanghai (Grant No. SSMU-ZDCX20180700), the Key Laboratory Program of the Education Commission of Shanghai Municipality (ZDSYS14005).

Authors' contributions

CZ conceived and designed the study. MW, JX, XL and BJ performed the experiments. YZ, CZ, SL and ZK performed data analysis. LJ, QL and CZ are responsible for writing and revising manuscript. All authors agreed on the final version of the manuscript.

Acknowledgements

We thank our laboratory colleagues for their assistance with experiments and

preparation of the manuscript.

References

1. Agulleiro MJ, Roy S, Sanchez E, Puchol S, Gallo-Payet N, Cerda-Reverter JM (2010) Role of melanocortin receptor accessory proteins in the function of zebrafish melanocortin receptor type 2. Mol Cell Endocrinol 320:145–152
2. Antal-Zimanyi I, Khawaja X (2009) The role of melanin-concentrating hormone in energy homeostasis and mood disorders. J Mol Neurosci 39:86–98

3. Asai M (2013) Loss of function of the melanocortin 2 receptor accessory protein 2 is associated with mammalian obesity (vol 341, pg 275, 2013). Science *341*, 959–959
4. Asai M, Ramachandrappa S, Joachim M, Shen Y, Zhang R, Nuthalapati N, Ramanathan V, Strochlic DE, Ferket P, Linhart K et al (2013) Loss of function of the melanocortin 2 receptor accessory protein 2 is associated with mammalian obesity. Science 341:275–278
5. Bohlooly YM, Mahlapuu M, Andersen H, Astrand A, Hjorth S, Svensson L, Tornell J, Snaith MR, Morgan DG, Ohlsson C (2004) Osteoporosis in MCHR1-deficient mice. Biochem Biophys Res Commun 318:964–969
6. Chaly AL, Srisai D, Gardner EE, Sebag JA (2016) The Melanocortin Receptor Accessory Protein 2 promotes food intake through inhibition of the Prokineticin Receptor-1. Elife *5*
7. Chan LF, Webb TR, Chung TT, Meimaridou E, Cooray SN, Guasti L, Chapple JP, Egertova M, Elphick MR, Cheetham ME et al (2009) MRAP and MRAP2 are bidirectional regulators of the melanocortin receptor family. Proc Natl Acad Sci U S A 106:6146–6151
8. Chen V, Bruno AE, Britt LL, Hernandez CC, Gimenez LE, Peisley A, Cone RD, Millhauser GL (2020) Membrane orientation and oligomerization of the melanocortin receptor accessory protein 2. J Biol Chem 295:16370–16379
9. Elliott JC, Harrold JA, Brodin P, Enquist K, Backman A, Bystrom M, Lindgren K, King P, Williams G (2004) Increases in melanin-concentrating hormone and MCH receptor levels in the hypothalamus of dietary-obese rats. Brain Res Mol Brain Res 128:150–159
10. Huszar D, Lynch CA, Fairchild-Huntress V, Dunmore JH, Fang Q, Berkemeier LR, Gu W, Kesterson RA, Boston BA, Cone RD et al (1997) Targeted disruption of the melanocortin-4 receptor results in obesity in mice. Cell
11. Jones BW, Song GJ, Greuber EK, Hinkle PM (2007) Phosphorylation of the endogenous thyrotropin-releasing hormone receptor in pituitary GH3 cells and pituitary tissue revealed by phosphosite-specific antibodies. J Biol Chem 282:12893–12906
12. Kokkotou EG, Tritos NA, Mastaitis JW, Slieker L, Maratos-Flier E (2001) Melanin-concentrating hormone receptor is a target of leptin action in the mouse brain. Endocrinology 142:680–686
13. Kowalski TJ, Spar BD, Weig B, Farley C, Cook J, Ghibaudi L, Fried S, O'Neill K, Del Vecchio RA, McBriar M et al (2006) Effects of a selective melanin-concentrating hormone 1 receptor antagonist on food intake and energy homeostasis in diet-induced obese mice. Eur J Pharmacol 535:182–191
14. Ranadive SA, Vaisse C (2008) Lessons from extreme human obesity: monogenic disorders. Endocrinol Metab Clin North Am *37*, 733–751, x
15. Rouault AAJ, Lee AA, Sebag JA (2017a) Regions of MRAP2 required for the inhibition of orexin and prokineticin receptor signaling. Biochim Biophys Acta 1864:2322–2329
16. Rouault AAJ, Rosselli-Murai LK, Hernandez CC, Gimenez LE, Tall GG, Sebag JA (2020a) The GPCR accessory protein MRAP2 regulates both biased signaling and constitutive activity of the ghrelin receptor GHSR1a. Science Signaling *13*

17. Rouault AAJ, Rosselli-Murai LK, Hernandez CC, Gimenez LE, Tall GG, Sebag JA (2020b) The GPCR accessory protein MRAP2 regulates both biased signaling and constitutive activity of the ghrelin receptor GHSR1a. Sci Signal *13*
18. Rouault AAJ, Srinivasan DK, Yin TC, Lee AA, Sebag JA (2017b) Melanocortin Receptor Accessory Proteins (MRAPs): Functions in the melanocortin system and beyond. Biochim Biophys Acta 1863:2462–2467
19. Sebag JA, Zhang C, Hinkle PM, Bradshaw AM, Cone RD (2013) Developmental control of the melanocortin-4 receptor by MRAP2 proteins in zebrafish. Science 341:278–281
20. Srisai D, Yin TC, Lee AA, Rouault AAJ, Pearson NA, Grobe JL, Sebag JA (2017) MRAP2 regulates ghrelin receptor signaling and hunger sensing. Nat Commun 8:713
21. Webb TR, Clark AJ (2010) Minireview: the melanocortin 2 receptor accessory proteins. Mol Endocrinol 24:475–484
22. Zhang LN, Sinclair R, Selman C, Mitchell S, Morgan D, Clapham JC, Speakman JR (2014) Effects of a specific MCHR1 antagonist (GW803430) on energy budget and glucose metabolism in diet-induced obese mice. Obesity (Silver Spring) 22:681–690

Figures

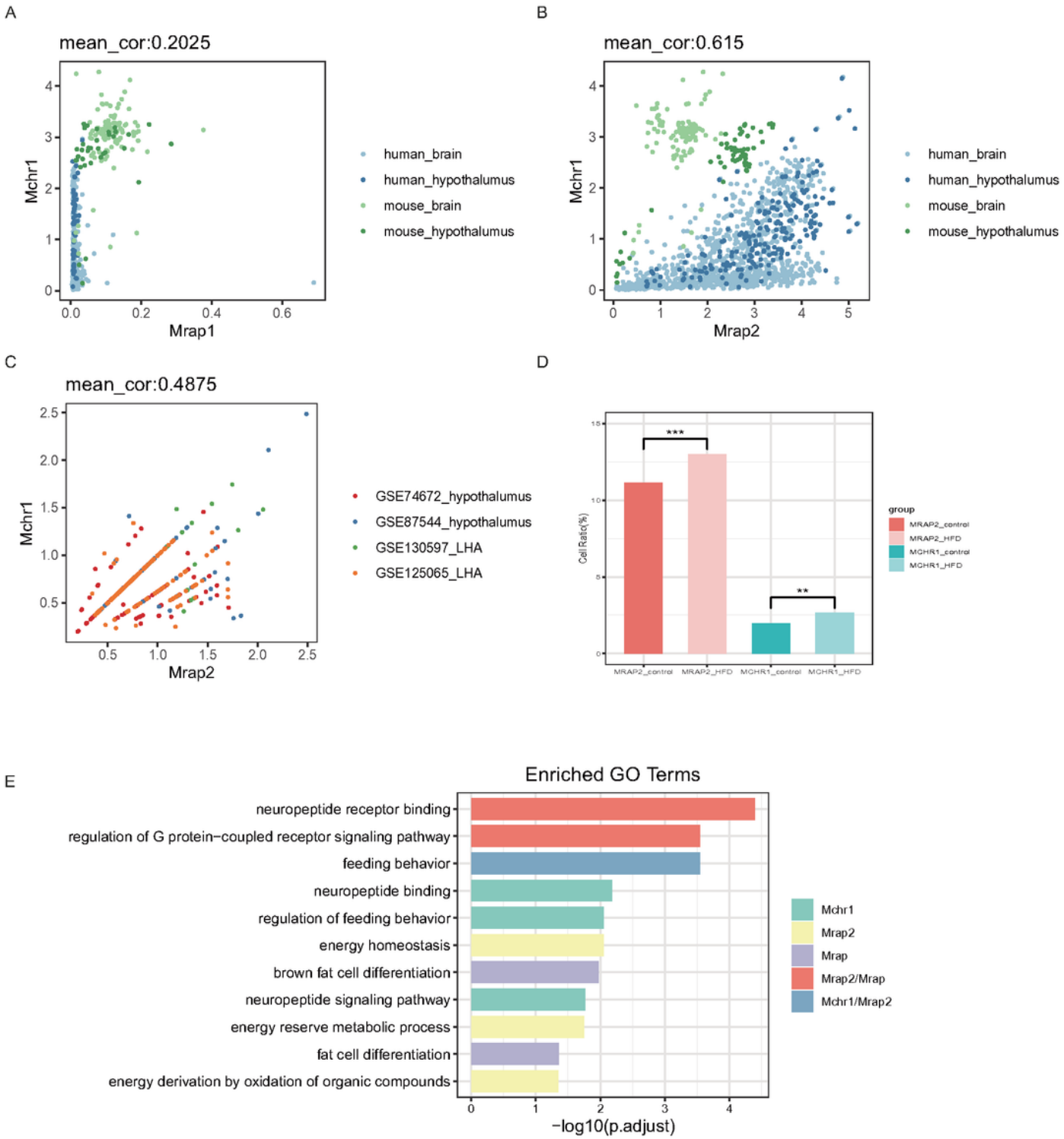

Figure 1

Co-expression and functional analysis of MCHR1 and MRAP proteins in human and mice RNA-seq datasets. (A-B) Co-expression correlation analysis of MRAP1 (A) or MRAP2 (B) with MCHR1 from the bulk RNA-seq data of human or mouse brain and hypothalamus. (C) Correlation coefficient between MRAP2 and MCHR1 from 4 single cell RNA-seq datasets of mouse hypothalamus. (D) Changes in cell proportion

of MCHR1 and MRAP2 in different metabolic states. (E) GO enrichment pathway analysis of MCHR1 and MRAP proteins.

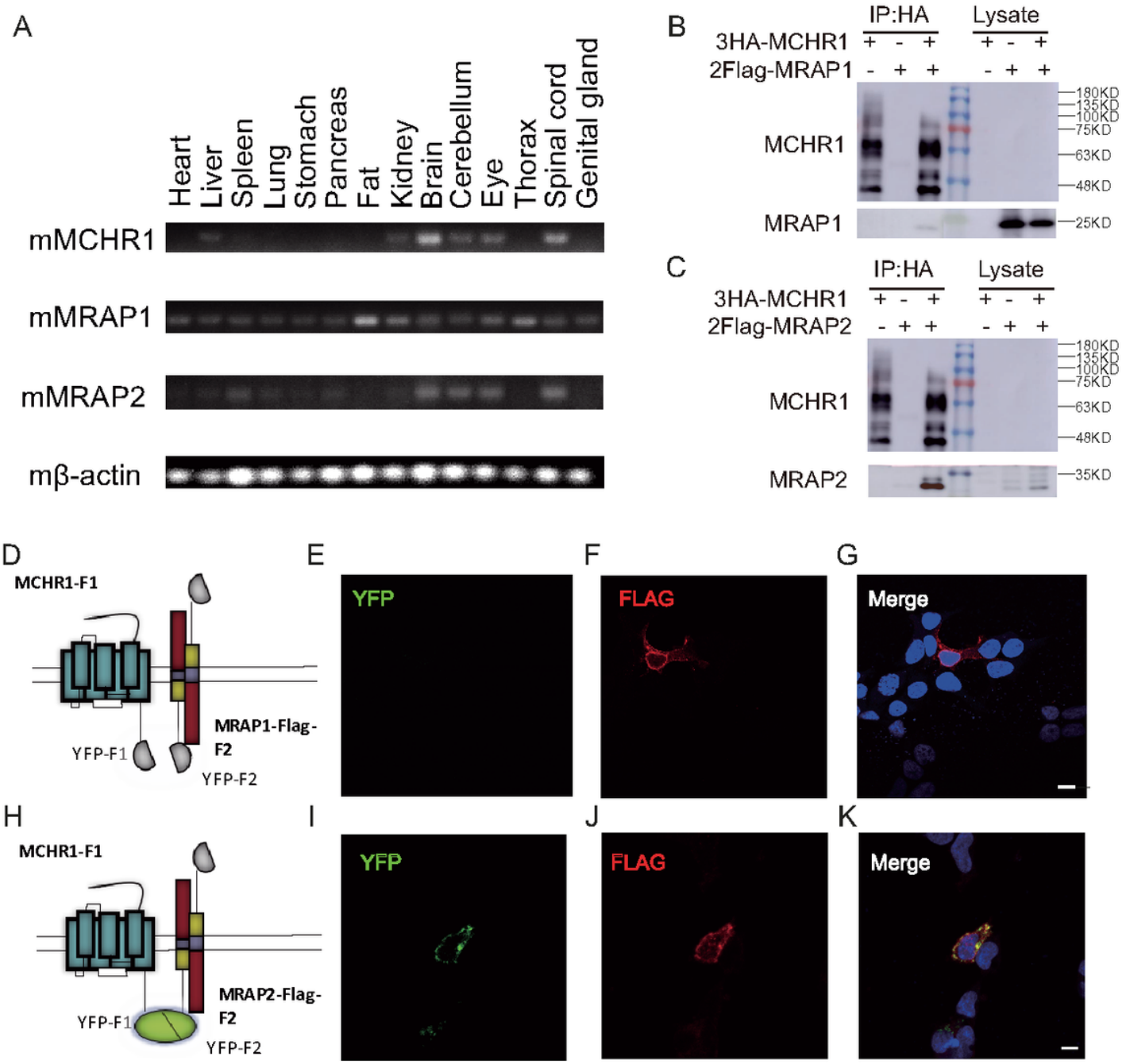

Figure 2

MCHR1 interact with MRAP2 but not MRAP1. (A) Tissue distribution of MCHR1, MRAP1 and MRAP2 tested by RT-PCR. β-actin was used as an internal control. (B-C) Co-IP shows interaction between 3HA-MCHR1 and 2Flag-MRAP1 (B) or 2Flag-MRAP2 (C). (D-K) MCHR1-F1 co-localizes with MRAP1-Flag- F2 (D-G) or MRAP2-Flag- F2 (H-K) in live cells. YFP fluorescence is exhibited in green (left panel). MRAP1 or MRAP2 in the same cells detected with anti-Flag antibody and secondary anti-mouse Alexa594 is shown

in red (middle panel). DAPI were applied to stain cell nuclei and shown in blue in merge figures (right panel). (Scale bars, 10 μm.)

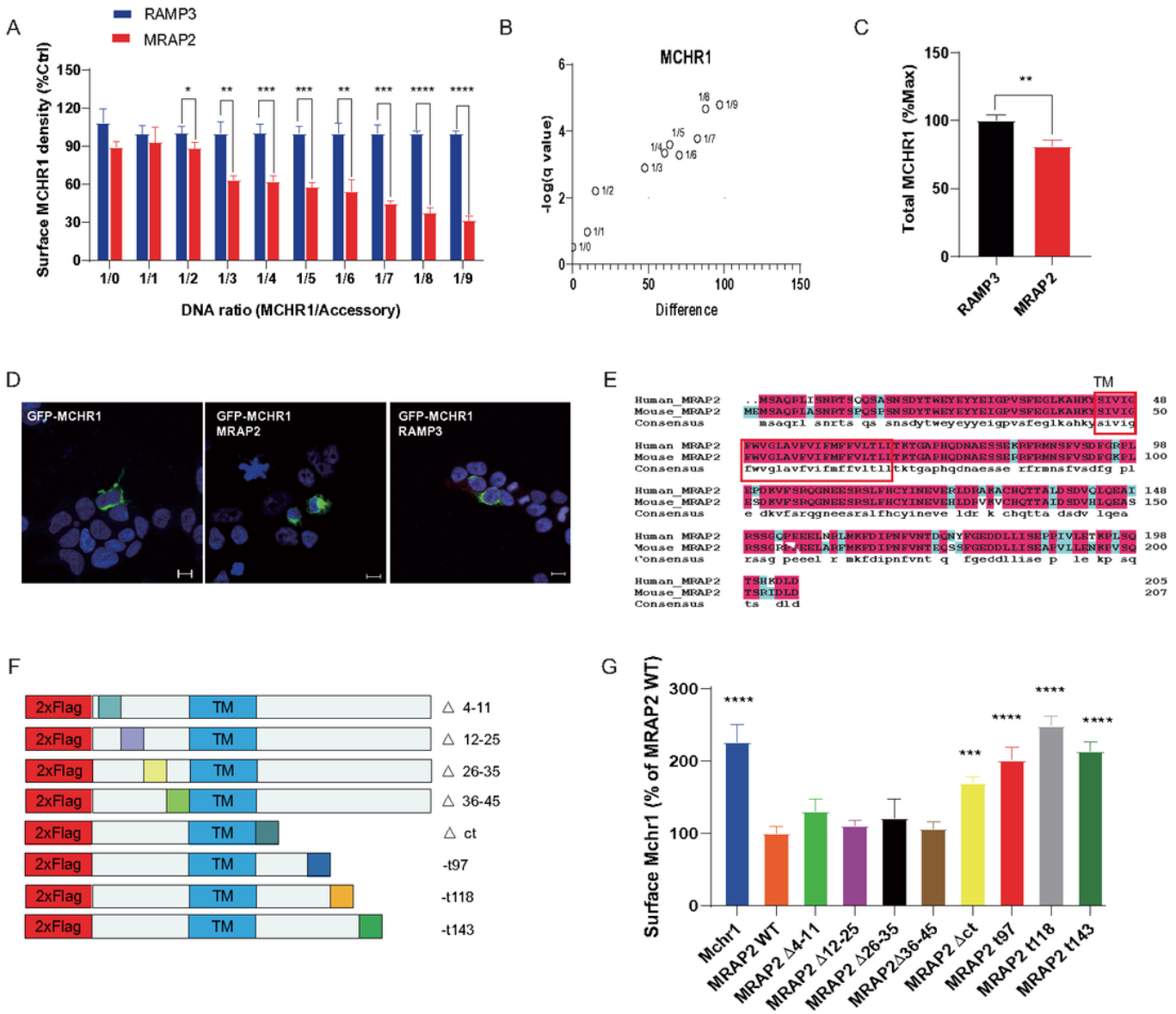

Figure 3

Regulation of MCHR1 trafficking by wt MRAP2 and its mutants. (A) Surface expression of MCHR1 measured by ELISA assay, which transfected with MRAP2 at different ratio (from 1:0 to 1:9). (B) D-value of MCHR1 membrane surface expression in the control group (RAMP3) and MRAP2 group at different transfection ratios. (C) Total expression of MCHR1 was also measured. (D) Localization of GFP-MCHR1 by confocal microscopy, which transfected with empty vector (left) or MRAP2 (middle) or RAMP3 (right). (E) Sequence alignment of human and mouse MRAP2. (F) Schematic representation of the MRAP2 mutants constructed. (G) The surface expression of MCHR1 when co-transfected with empty vector

(control), wt MRAP2 or different mutants. One-way ANOVA with post hoc Tukey test. ns (no significant change), *p<0.05, **p<0.01, ***p<0.001,****p<0.0001.

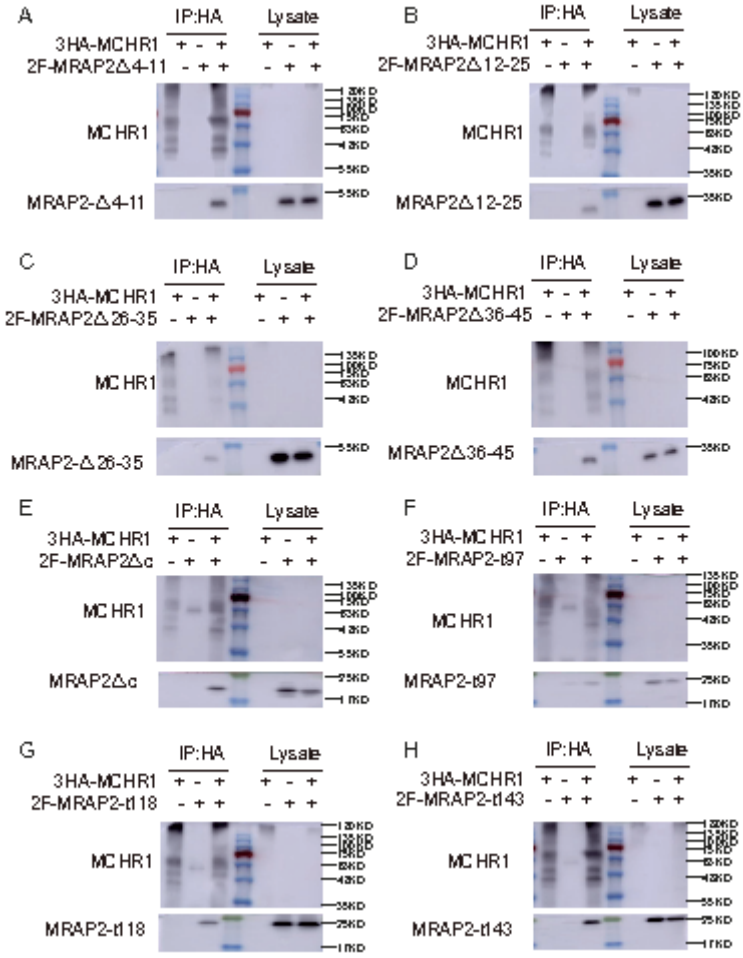

Figure 4

Interaction between 3HA-MCHR1 and MRAP2 mutants. (A-D) MRAP2 C-terminal mutants; (E-H) MRAP2 N-terminal mutants. Middle lane with color is protein marker in all figures.

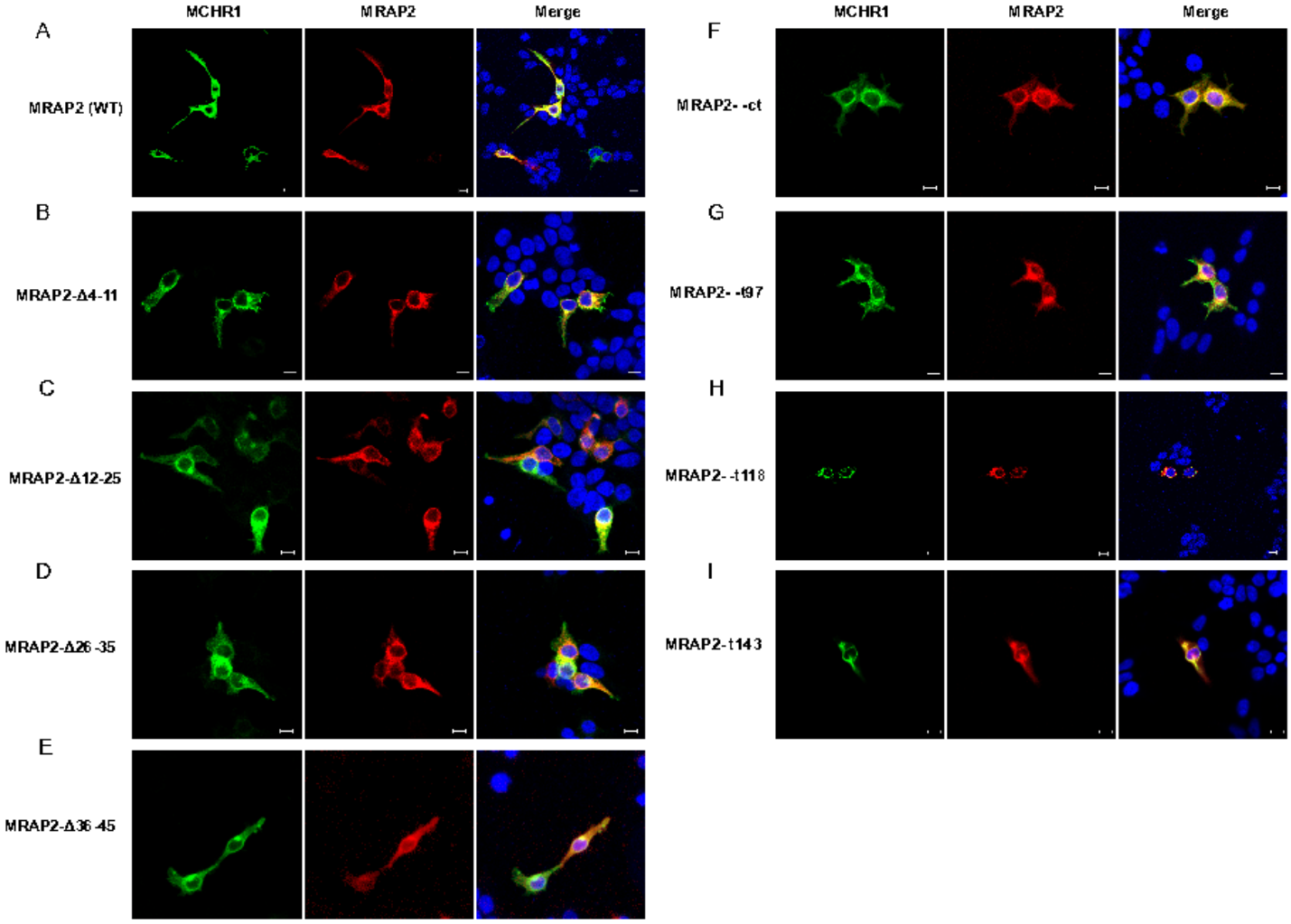

Figure 5

Co-localization of MRAP2 mutants with MCHR1. Localization of MCHR1 (green) when co-transfected with wt MRAP2 or indicated MRAP2 mutants (red). Images in A are transfected with wt MRAP2; images in B-E are MRAP2 C-terminal mutants; F-I are MRAP2 N-terminal mutants. DAPI was used to stain cell nuclei and shown in blue. Co-localized MRAP2 and MCHR1 of merged images are shown in yellow.

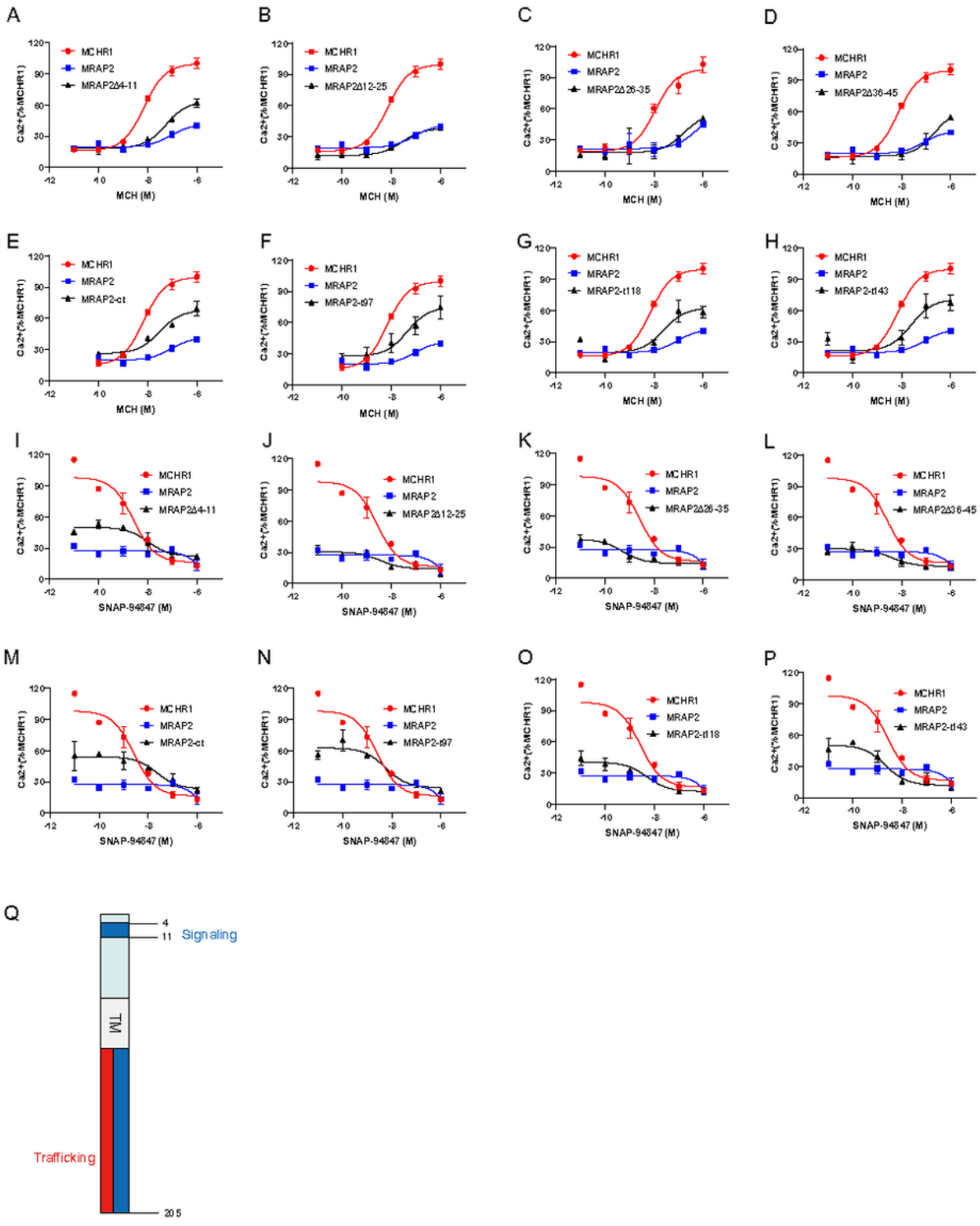

Figure 6

The influence of MCHR1 signaling by the functional domains of MRAP2. (A-H) Calcium response of MCHR1 simulated by increasing concentrations of MCH, transfected with wt MRAP2 or indicated mutants. (I-P) Competition binding assay of MCHR1 in 293T cells transfected with wt MRAP2 or indicated mutants. Relative luminescence intensity of NFAT-luc represents the normalized NFAT-luc units to p-RL-TK units (transfected internal control). Each data point represents the mean ± SEM of three

replicates (N = 3). (Q) Schematic diagram of distinct regions of MRAP2 required for regulating the trafficking and signaling of MCHR1.